PHOTOCATALYTIC DEGRADATION OF PHENOL BY SILICA GEL-SUPPORTED TITANIA NANOTUBES

BY

WONG CHUNG LENG

Thesis submitted in fulfillment of the

degree of

Master of Science

2012

ACKNOWLEDGEMENTS

First and foremost, I would like to express my sincere appreciations to my beloved parents, Mr. Wong Sing Hie and Mdm. Tang Kin Chuo and family. Without their patient and encouragement, this thesis would not have been possible. I sincerely appreciate invaluable support and caring I received from them throughout this thesis.

I would also like to express my gratefulness to my supervisor, Professor Abdul Rahman Mohamed for his valuable supervision and guidance. His valuable comments and assistances helped me to improve the thesis in many ways.

I also respectfully acknowledge all the lecturers, staffs and technicians, School of Chemical Engineering at Universiti Sains Malaysia (USM) for giving me their valuable time to guide me throughout my higher education. Additionally, I would thank to the technicians of School of Biology Science and School of Material and Mineral Resources, USM for the sample analysis.

I would like to acknowledge the economic support received from USM, through the USM Fellowship, Postgraduate Research Grant Scheme (no. 8033054), and Fundamental Research University Grant Scheme (no. 811068).

Last but not least, I would like to express my sincere gratitude to all my friends for the help and moral support throughout this Master study.

TABLE OF CONTENTS

LIST OF TABLES

LIST OF FIGURES

Page

LIST OF SYMBOLS

Symbol	Description	Unit
ΔE_g	Band gap energy	eV
C	Concentration of phenol	mg/L
C_o	Initial phenol concentration	mg/L
C_w	Concentration of water	mg/L
$C_6H_6O^-$	Phenolate anions	-
Cl^-	Chloride ion	-
$Cl\cdot$	Chloride radical	-
$CO_3^{-}\cdot$	Carbonate radical ion	-
D	Crystallite size	nm
e^-	Electron	-
Fe^{2+}	Ferum (II) ion	-
h^+	Positive hole	-
h_v	Energy required to transfer the excited electron from the valence band to the empty conduction band	eV
H^+	Hydrogen ion	-
HCO_3^-	Bicarbonate ion	-
$HO\cdot$	Hydroxyl radical	-
$HO_2\cdot$	Hydroperoxyl radical	-
k	Reaction rate constant	mg/L.s
		mg/L.min
k_{app}	Apparent rate constant	1/min
$k_{HO\cdot}$	Reaction rate constant of hydroxyl radical	mg/L.s
K	Adsorption constant	L/mg

Symbol	Description	Unit
K_w	Water adsorption constant	L/mg
Na^+	Sodium ion	-
O^+	Oxidation product	-
$O_2\cdot^-$	Superoxide radical anion	-
OH^-	Hydroxyl ion	-
r	Reaction rate	mg/L.min
r_o	Initial reaction rate	mg/L.min
R	Reacting organic compounds	-
R^2	Correlation coefficients	-
R^2_{adj}	Adjusted correlation coefficients	-
ROH	Olefins or aromatic compounds	-
SO_4^{2-}	Sulphate ion	-
$SO_4^{-}\cdot$	Sulphate radical ion	-
t	Time	min
$(Ti_3O_7)^{2-}$	Tri-titanate	-

Greek symbol

Symbol	Description	Unit
ε	Error	-
2θ	Diffraction angle	°
θ	Fractional site coverage	molecule/nm^2
λ	Wavelength of the X-ray radiation	nm
β	Full width at half-maximum height	°

LIST OF ABBREVIATIONS

2-CP	2-chlorophenol
2FI	Two factorial interaction
4-NP	4-nitrophenol
AC	Activated carbon
ACGIH	American Conference of Governmental Industrial Hygienists
Adq. Precision	Adequate precision
ANOVA	Analyses of variance
AO7	Acid orange 7
AOPs	Advanced oxidation processes
BBD	Box-Behnken design
BEI	Back scattering electron imaging
BET	Brunauer-Emmett-Teller
CCC	Central composite circumscribed
CCD	Central composite design
CCF	Central composite face centered
CCI	Central composite inscribed
CdS	Cadmium sulfide
CdSe	Cadmium selenide
CFD	Computational fluid dynamics
$C_6H_5C(CH_3)_2OOH$	Cumene hydroperoxide
$C_6H_5CH(CH_3)_2$	Cumene
C_6H_5Cl	chlorobenzene
C_6H_5ONa	Sodium phenolate
$C_6H_5SO_3H$	Benzenesulfonic acid

$C_6H_5SO_3Na$	Sodium benzenesulfonate
C_6H_6	Benzene
$CH_3(CH)CH_2$	Prop-1-ene
$(CH_3)_2CO$	Acetone
CO_2	Carbon dioxide
Cu_2O	Copper oxide
C.V.	Coefficient of variation
DF	Degree of freedom
DIOX	1, 4-dioxane
DOE	Department of environmental
EDX	Energy dispersive X-ray spectroscopy
EOP	Electrochemical oxidation potential
EPA	Environmental Protection Agency
ETBE	Ethyl tert-butyl ether
Fe_2O_3	Iron (III) oxide
F value	Fisher value
GAC	Granular activated carbon
Ge	Germanium
HCl	Hydrochloric acid
H_2O	Water
H_2O_2	Hydrogen peroxide
H_2SO_4	Sulphuric acid
$H_2Ti_3O_7$	Hydrogen trititanate
$H_2Ti_3O_7 \cdot nH_2O$ (n< 3)	Hydrated hydrogen titanate
HPLC	High pressure liquid chromatograph

IUPAC	International union of pure and applied chemistry
L-H	Langmuir-Hinshelwood
MWCNTs	Multi-walled carbon nanotubes
Na	Sodium atom
NaCl	Sodium chloride
$NaHCO_3$	Sodium bicarbonate
NaOH	Sodium hydroxide
Na_2SO_3	Sodium sulfite
Na_2SO_4	Sodium (II) sulfate
$Na_2Ti_3O_7$	Sodium metatitanate
NIOSH	National Institute for Occupational Safety and Health
O	Oxygen atom
O_2	Oxygen molecules
O_3	Ozone
OSHA	Occupational Safety and Health Administration
PbS	Lead (II) sulfide
Prob > F	Probability value greater than Fisher value
PTFE	Polytetrafluoroethene
pzc	Zero point charge
RSM	Response surface methodology
SEI	Secondary electron imaging
Si	Silicon atom
SiO_2	Silica
SnO_2	Tin oxide
SNTZS	Supported nano-TiO_2/ZSM-5/silica gel

SO_2	Sulfur dioxide
Std. Dev.	Standard deviation
TEM	Transmission electron microscopy
THF	Tetrahydrofuran
Ti	Titanium atom
TiO_2	Titanium dioxide
TiOH	Titanol surface group
TOC	Total organic carbon
TWA	Time-weighted average
UV	Ultraviolet
WO_3	Tungsten oxide
XRD	X-ray diffractometer
ZnO	Zinc oxide
ZnS	Zinc sulphide
ZrO_2	Zirconium dioxide
ZSM-5	Zeolite

DEGRADASI PEMFOTOMANGKINAN FENOL DENGAN MENGGUNAKAN NANOTIUB TITANIA DIIMOBILISASI PADA GEL SILIKA

ABSTRAK

Nanotiub TiO_2 dan nanotiub TiO_2 yang tersekat gerak telah berjaya disintensiskan oleh kaedah hidroterma dan kaedah pengikatan. Fotomangkin-fotomangkin yang dihasilkan telah dikaji dengan menggunakan kaedah Brunauer-Emmett-Teller (BET), mikroskop elektron pengimbasan (SEM), penyebaran elektron sinar-X (EDX), mikroskop elektron transmisi (TEM) dan pembelauan sinar-X (XRD). Aktiviti-aktiviti pemfotomangkinan bagi fotomangkin-fotomangkin diselidik melalui degradasi pemfotomangkinan fenol dalam larutan berair di dalam reaktor kelompok. Nanotiub TiO_2 yang dihasilkan pada 130 °C selama 3 jam menunjukkan kadar degradasi fenol tertinggi berbanding dengan sampel-sampel lain yang disediakan pada 130 °C selama 1 jam, 5 jam and 7 jam. Degradasi lengkap telah dicapai oleh sampel yang dihasilkan pada 130 °C selama 3 jam dalam 130 minit. Tumpuan khusus telah diberikan untuk menentukan komposisi optimum bagi setiap komponen (pemangkin, sokongan dan pengikat) dalam pengimobilisasian nanotiub TiO_2. Keberkesanan degradasi fenol yang tertinggi telah dicapai ketika nisbah nanotiub TiO_2: gel silika: koloid silika ialah 1:2:20. Nanotiub TiO_2 dan nanotiub TiO_2 yang tersekat gerak menunjukkan aktiviti pemfotomangkinan yang lebih tinggi dibandingkan dengan TiO_2 tulen. Aktiviti pemfotomangkinan bagi nanotiub dan nanotiub TiO_2 yang tersekat gerak mencapai degradasi fenol sebanyak 100 % dan

98.0 % masing-masing, manakala TiO_2 tulen hanya mencapai 77.0 % degradasi. Selain itu, kecekapan pemfotomangkinan bagi nanotiub TiO_2 yang terimobilisasi adalah menurun dengan sedikit selepas degradasi fenol selama empat kali. Kehilangan peratusan degradasi pemfotomangkinan adalah kurang daripada 2 % walaupun selepas empat kitaran. Keputusan untuk pembolehubah proses yang dikaji adalah: anion menunjukkan kesan negatif pada degradasi fenol dalam turutan $SO_4^{2-} > Cl^- > HCO_3^-$; nilai pH yang optimum ialah pH 5.5 (pH semula jadi); kadar aliran udara yang optimum adalah 0.3 L/min; degradasi fenol merosot bagi peningkatan kepekatan awal fenol. Rekabentuk ujikaji metodologi permukaan sambutan (RSM) berdasarkan kepada reka bentuk gabungan berpusat (CCD) telah digunakan untuk mengoptimumkan dan meramalkan interaksi antara pembolehubah proses dengan meminimumkan jumlah dan masa untuk penjalanan eksperimen. Akhirnya, kinetik degradasi fenol dengan nanotiub TiO_2 yang terimobilisasi mematuhi model Langmuir-Hinshelwood. Nilai pemalar kadar, k dan nilai pemalar jerapan, K yang telah diperolehi adalah 0.9324 mg/L.min dan 0.0121 L/mg masing-masing.

PHOTOCATALYTIC DEGRADATION OF PHENOL BY SILICA GEL-SUPPORTED TITANIA NANOTUBES

ABSTRACT

TiO_2 nanotubes and immobilized TiO_2 nanotubes were successfully synthesized by a hydrothermal method and binding method. The produced photocatalysts were characterized by the Brunauer-Emmett-Teller (BET) method, scanning electron microscopy (SEM), energy dispersive X-ray spectroscopy (EDX), transmission electron microscope (TEM) and X-ray diffraction (XRD). The photocatalytic activities of the photocatalysts were evaluated through the photocatalytic degradation of aqueous phenol solution in a batch reactor. TiO_2 nanotubes produced at 130 °C for 3 h showed the highest degradation rate of phenol compared with the other samples prepared at 130 °C for 1 h, 5 h and 7 h, complete degradation being achieved in 130 min. Special focus was given in order to determine the optimum composition of each component (catalyst, support and binder) in the immobilization of TiO_2 nanotubes. The highest efficiency of phenol degradation was achieved when the ratios of TiO_2 nanotubes: silica gel: colloidal silica was 1:2:20. For the comparison, TiO_2 nanotubes and immobilized TiO_2 nanotubes showed higher photocatalytic activity as compared with pure TiO_2. The photocatalytic performance of TiO_2 nanotubes and immobilized TiO_2 nanotubes achieved 100 % and 98.0 % respectively, of phenol degradation, whereas pure TiO_2 attained only 77.0 % degradation. The photocatalytic activity of the immobilized TiO_2 nanotubes was slightly decreased after four cycles for phenol degradation. The

loss in percentage of photocatalytic degradation was less than 2 % even after four cycles. The results for the studied operating parameters were: the presence of the anions were found to inhibit the photocatalytic degradation of phenol in the order of $SO_4^{2-} > Cl^- > HCO_3^-$; the optimal medium pH was found to be pH 5.5 (natural pH); the air flow rate gave an optimum value of 0.3 L/min; the phenol degradation efficiency decreased as initial phenol concentration increased. Response surface methodology (RSM) based on the central composite design (CCD) was used to optimize and predict the interactions between process variables by reducing the numbers and the times for the experimental runs. Finally, the reaction kinetics of phenol degradation by the immobilized TiO_2 nanotubes obeyed well with the Langmuir-Hinshelwood model. The values of the reaction rate constant, k and the adsorption constant, K obtained were found to be 0.9324 mg/L.min and 0.0121 L/mg, respectively.

CHAPTER 1

INTRODUCTION

1.1 Treatment of Industrial Effluent

In urban and agricultural industries, industrial wastewater treatment is of great concern for the degradation and removal of contaminants. Noteworthy among the variety of industries activities are milling and coal conversion, organic chemicals and synthetic industries and textile processing industries, not to mention the pollution emanating from the use of fuel for heating and transportation and from agricultural and domestic use of fertilizers, pesticides and detergents (Serpone, 1995). A research conducted in USA shows that 80 % of organic contaminants present in streams (Bódalo et al., 2008). Among these, phenol and phenolic compounds are the major organic contaminants in industrial wastewaters (Bódalo et al., 2008).

In Malaysia, the number of water pollution sources was reported to 20,702 sources in 2009. A total of 9,762 sources were identified with manufacturing industries having the highest number of water pollution sources. Otherwise, based on the notification of scheduled waste received by the Department of Environmental (DOE), a total of 1,705,308.14 metric tons of scheduled waste were generated in 2009 as compared to 1,304,898.77 metric tons in 2008. It was found that 5,591.19 metric tons of phenol/adhesive/resin were produced in the country in 2009 (DOE, 2009).

Several conventional techniques for the removal of organic pollutants from wastewaters include adsorption, air stripping, biological methods, coagulation, extraction, incineration, oxidation via ozonation or via hydrogen peroxide and ultrafiltration (Serpone, 1995; Mahmoodi and Arami, 2009). However, these approaches do not effectively break down or degrade the organic pollutants in wastewater. These are slow processes because the complete biodegradation of organic pollutants requires several days or weeks. Moreover, at high concentrations of organic pollutants, these approaches present some shortcomings during operation (Laoufi et al., 2008).

Although the adsorption treatment has always been efficient to control the biochemical oxygen demand (Lee et al., 2008a), it transfers the organic pollutants from water to another medium, and hence, contributing to secondary pollution (Laoufi et al., 2008; Mahmoodi and Arami, 2009). Otherwise, the organic pollutants are required to be treated first before the adsorption process. For the re-use purpose, the adsorbents have to be regenerated at the end of adsorption process (Mahmoodi and Arami, 2009). Air stripping is often ineffective in degrading organic pollutants because it also simply transfers the organic pollutants from water to another phase (Serpone, 1995). Conventional biological methods are not suitable in removing and degrading the organic pollutants because mostly the aromatic rings in the organic pollutants are physically and chemically stable, hence, the degradation process using conventional biological method is normally selective and incomplete (Mahmoodi and Arami, 2009). Ozonation is not suitable in removing or degrading the organic pollutants due to its high operating cost. Lastly, coagulation treatment is inexpensive because it simply uses alums, limes and ferric salts, however, it poses waste disposal problems after the coagulation treatment (Mahmoodi and Arami, 2009).

In this way, efficient, environmentally benign and low cost approaches for the degradation and removal of organic pollutants have been focused of current research to control the water quality (Kashif and Feng, 2009).

1.2 Heterogeneous Photocatalysis in Wastewater Treatment

To improve the wastewater pollutants degradation, advanced oxidation processes (AOPs) using titanium dioxides (TiO_2) have been applied in the decontamination, mineralization and oxidation of the organic pollutants in wastewater without contributing secondary pollutions. The heterogeneous photocatalysis has been focused as a new air and water purification method since the photocatalytic splitting of water was discovered by Honda and Fujishima using TiO_2 electrodes in 1972 (Yu et al., 2007a). The heterogeneous photocatalysis has attracted much attention because of its advantages: (1) complete degradation or mineralization of contaminants to mineral acids, water and carbon dioxide by irradiating TiO_2 under ultraviolet (UV) light, (2) operated at mild temperature and pressure and (3) no waste-solids disposal problem.

Also, TiO_2 has demonstrated advantages that include photochemical stability, biologically and chemically inert, non-toxic, cheap, widespread availability and wide band gap (Liu et al., 2008; Mahmoodi and Arami, 2009). Consideration attempts have been taken in the development of titanium dioxide photocatalysts for environmental protection procedures such as air purification, water purification, disinfection, antibacterial protection, hazardous waste remediation and treatment of harmful gas emission (Yu et al., 2007a). Hence, significant improvement and optimization of titanium dioxide photocatalysts are required to improve its low photocatalytic efficiency in the present day photooxidation technology. The

optimization and improvement of the photocatalytic performance of TiO_2 is mainly focused in the TiO_2 production via different chemical and physical methods in order to improve its crystallite phase, dimension and morphology (Lee et al., 2007).

In addition, the disadvantages of using suspended TiO_2 in photocatalytic processes include (1) the large usage of TiO_2 semiconductor photocatalysts, (2) the problems encountered in recycling TiO_2 semiconductor photocatalysts, (3) difficulty in TiO_2 semiconductor photocatalysts recovery using centrifugation and filtration and (4) the agglomeration of TiO_2 semiconductor photocatalysts (Mahmoodi and Arami, 2009). Owing to the high stability and small size of TiO_2 semiconductor photocatalysts, the recovery of TiO_2 semiconductor photocatalysts are difficult to perform at the end of the photocatalytic reaction (Costa and Prado, 2009). When TiO_2 semiconductor photocatalysts agglomerate into larger particles, they have an inclination to decrease their effective surface area and photocatalytic efficiency (Ribbens et al., 2008). Therefore, the agglomeration problems result to the complications in the disposal problems and the recombination of photogenerated electron-hole pairs. On the other hand, the strong photocatalytic absorptions limit the depth of UV penetration, which led to the low photocatalytic activity in the organic pollutants removal (Kashif and Feng, 2009; Mahmoodi and Arami, 2009).

Hence, the above problems can be solved in order to improve photocatalytic efficiency of TiO_2 by the immobilization of photocatalysts over suitable supports such as silica, alumina, zeolite or clay and activated carbon. However, after the immobilization process, the overall photocatalytic activity of immobilized TiO_2 may lower than suspended TiO_2 due to the mass transfer limitation and surface area reduction. The electron-hole recombination reaction on the surface may thus increase,

hence, decreasing the degradation rate of organic pollutants (Kashif and Feng, 2009; Mahmoodi and Arami, 2009).

Beside the immobilization method, different preparations of TiO_2 nanostructures are being carried out with the purpose of increasing photocatalytic efficiency (Costa and Prado, 2009; Okour et al., 2009). The new opportunities and features of one dimensional TiO_2 nanostructures (nanofibers, nanowires and nanotubes) have attracted much attention in many promising applications (Costa and Prado, 2009). They present excellent physicochemical properties for the improved performance in catalyst supports, dye-sensitized solar cells, electronic devices and photocatalysis.

Several researches have stated that tube-like structure possess better chemical and physical in photocatalytic reaction compared with other form of TiO_2 nanostructures. Consequently, TiO_2 nanotubes present high pore volume and specific surface area, high photocatalytic activity and excellent mechanical and electronic properties. The photocatalytic performance of the photocatalysts is then improved with these excellent present properties. There are many techniques to synthesize the nanotubes such as anodizaiton, chemical vapor deposition, electrochemical synthesis and sol-gel method. Among these, TiO_2 nanotubes synthesized by a simple hydrothermal method has gained much attention in nanotechnology because of its many advantages like low cost, low energy consumption, mild reaction condition and simplicity (Wang et al., 2008a). However, a large number of variable factors such as the preparation conditions (pH, acid concentration, starting materials, hydrothermal reaction temperature and duration) are needed to manipulate to control the morphology of TiO_2 nanotubes with high surface area and pore volume.

1.3 Problem Statement

TiO_2 is a promising photocatalyst in many environmental applications especially in the organic pollutant treatments. It has been applied in the photocatalytic reaction because of its water insoluble, inexpensive and non-toxic. However, there are practical restrictions for its wide practical application in photocatalytic processes, which are (1) the small percentage of photons of the solar radiation, which only the thin exterior layer of the unsupported photocatalyst actually absorbs UV light; (2) high charge recombination rate of the photogenerated electrons and holes and (3) the photocatalyst removal problem. Those problems can be overcame by immobilization of TiO_2 nanotubes with various supports, such as, aluminium sheets, ceramics, glass rings, silica, magnesia and others. Even though immobilized TiO_2 nanotubes allows the easily continuous use of the photocatalysts by reducing the need of additional separation processes in a slurry system, there are still technical challenges that must be further observed and solved. Preparation of immobilized TiO_2 nanotubes is important to compensate to the reduced performances associated with the immobilization process owing to its high pore volume and surface area and consistent with a high volume fraction of active sites located on the surface for substrate adsorption.

As most commonly known, various techniques like anodizaiton, chemical vapor deposition, electrochemical synthesis and sol gel method are prominent methods for the synthesis of TiO_2 nanotubes. However, most of them are expensive, high energy consumption, complex equipment requirement and not commercially viable for the large scale production. To avoid these effects, hydrothermal method has been considered as an alternative approach in the synthesis of TiO_2 nanotubes, where the crystallite phase, grain size, surface chemistry and particle morphology

can be controlled by preparation parameters like aging duration, addition of additives, hydrothermal treatment duration and temperature, pH, nature of solvent and sol composition. Normally, different characteristics and morphologies of TiO_2 nanotubes are formed under various hydrothermal conditions. Thus, in this research, the effect of the hydrothermal reaction duration is focused to investigate in order to prepare the well-crystalline, dispersed and uniform TiO_2 nanotubes and to improve its activity and efficiency to remove the phenol.

Otherwise, an effective reactor design is important in the photocatalysis where intimate contact can be achieved between UV light, photocatalyst and organic pollutant. The operation of batch reactor can increase the photocatalytic efficiency owing to its excellent reactant contact, efficient UV light irradiation and high photocatalyst loading. However, the technical development is still under investigation in heterogeneous photocatalysis for the wastewater treatment. Thus, a detailed study on the effect of operating parameters is taken to investigate the photocatalytic performance of the prepared photocatalysts in the batch reactor. The importance of the present work is to exploit the wide and ever-growing application of photocatalysts to be more practical in the wastewater treatment by studying the factors in the synthesis of TiO_2 nanotubes and supported TiO_2 nanotubes with their photocatalytic performance in a batch reactor.

1.4 Research Objectives

The main objective of this study is to synthesize TiO_2 nanotubes and immobilized TiO_2 nanotubes capable of degrading phenol under UV irradiation. More specifically we attempted:

1. To synthesize and characterize TiO_2 nanotubes prepared via hydrothermal method under different hydrothermal reaction duration (1-7 h).
2. To immobilize TiO_2 nanotubes onto silica gel using a simple binding method and characterize the selected optimal immobilized TiO_2 nanotubes.
3. To investigate the process parameters on the phenol degradation using immobilized TiO_2 nanotubes in a batch reactor.
4. To optimize the process conditions for phenol degradation using immobilized TiO_2 nanotubes.

   This optimization process is based on response surface methodology (RSM) which has three parameters: TiO_2 nanotubes loading, initial phenol concentration and air flow rate.
5. To analyze kinetic parameters of the photocatalytic degradation of aqueous phenol solution in the batch reactor.

   The initial phenol concentration is used as kinetic parameter in this research and its analysis is based on the Langmuir-Hinshelwood kinetic model.

1.5 Research Scope

A flow diagram for the whole study in this research is shown in Figure 1.1. The research is mainly focused on the formation of highly photocatalytic activity TiO_2 nanotubes via a simple hydrothermal approach. The effect of hydrothermal reaction time (1-7 h) was studied in the formation of TiO_2 nanotubes using hydrothermal method. The characterizations of the prepared photocatalyst are analyzed using X-ray diffraction (XRD), energy dispersive X-ray spectroscopy (EDX), Brunauer-Emmett-Teller (BET) and transmission electron microscopy (TEM). The photocatalytic degradation performance of photocatalysts is evaluated through the photocatalytic degradation of aqueous phenol solution in a batch reactor.

Next, TiO_2 nanotubes supported on silica gel were prepared using a simple binding method. The morphology of the supported TiO_2 nanotubes is characterized using scanning electron microscopy (SEM), X-ray diffractometer (XRD) and the Brunauer-Emmett-Teller (BET) technique. Various process variables such as TiO_2 nanotubes loading (0.30-1.50 g/L), silica gel loading (0.50-2.00 g/L), colloidal silica loading (2.00-14.00 g/L), pH solution variation (pH 3, 5.5, 7 and 9), inorganic anions (Cl^-, HCO_3^- and SO_4^{2-} ions), air flow rate (0-0.5 L/min) and initial phenol concentration (10-90 mg/L) are studied to investigate the photocatalytic performance of photocatalysts in batch reactor.

Response surface methodology (RSM) is used to optimize and analyze the possible interaction between the operating parameters and the percentage of phenol degradation. The selected variables are TiO_2 nanotubes loading (0.30-0.70 g/L), initial phenol concentration (10-50 mg/L) and air flow rate (0.1-0.5 L/min). Design of Experiment using Design-Expert (version 6.0.6, StatEase, Inc., USA) was used in the RSM. The reaction kinetics parameters are further studied based on the

Langmuir-Hinshelwood kinetic model. The rate of reaction is determined based on initial phenol concentration as kinetic parameter in the photocatalytic degradation of aqueous phenol solution.

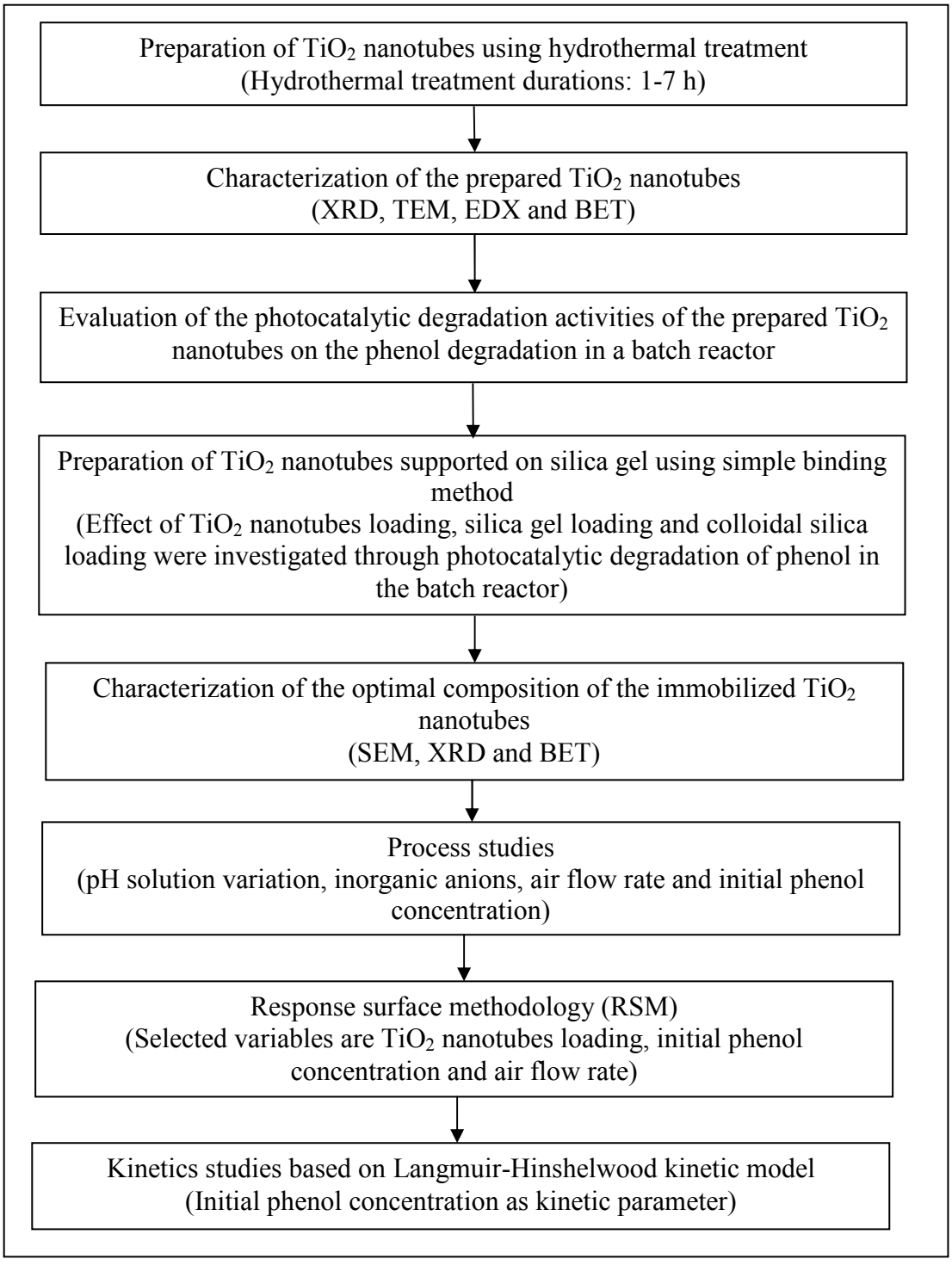

Figure 1.1 A Process Flow Chart of the Research Activities.

1.6 Organization of Thesis

This thesis is made up of five chapters that cover important details regarding the research. Chapter 1 (Introduction) includes a brief discussion on the water treatment and heterogeneous photocatalysis. This chapter also includes the problem statement that relates the problem faced and the needs of the current research. The research objectives and research scopes are conducted throughout the research.

Chapter 2 consists of the literature review related on the photocatalysis field. A brief explanation about the advanced oxidation process and heterogeneous photocatalysis is in the first part. Next, the information regarding with TiO_2 as a photocatalyst, nanostructured TiO_2, techniques for the production of TiO_2 nanotubes, formation mechanism of TiO_2 nanotubes, importance of the immobilization of TiO_2 nanotubes and batch reactor are also discussed as they play an important roles wherein the reaction takes place. The introduction of the phenol is included in this part. The effects of various operating parameters (photocatalyst loading, medium pH and initial phenol concentration) that affect the photocatalytic activity are included. The final part of this chapter is a short review of the design of experiment (DOE) including the response surface methodology (RSM). It was used to analyze and optimize the operating parameters in the photocatalytic degradation of aqueous phenol solution.

Chapter 3 (Experimental) covers all experimental work. Details of the materials and chemical reagents used with a general description are prepared in a table for easy identification. A thorough description of the Teflon-lined autoclave and batch reactor is described in this chapter. The detailed of the preparation of photocatalysts and characterization methods are conducted throughout this research. Lastly, the process studies and experimental design are discussed in this chapter.

All the results and discussions related to the current research work are presented in Chapter 4. It is divided into parts: (1) Characterization results of TiO_2 nanotubes and immobilized TiO_2 nanotubes; (2) Preliminary studies; (3) Effect of operating parameters on the photocatalytic degradation of aqueous phenol solution in a batch reactor; (4) Optimization studies using response surface methodology (RSM); and (5) Reaction kinetic parameters from the Langmuir-Hinshelwood kinetic model representing the degradation rate of phenol over different concentrations.

Chapter 5 gives the overall conclusion based on the results obtained throughout the current study as previously discussed in Chapter 4. Some recommendations for future studies are also included as a continuation for the present one.

CHAPTER 2

LITERATURE REVIEW

This chapter reviews background information on the photocatalysis that leads to this research work. It begins with the advanced oxidation processes, heterogeneous photocatalysis, properties of TiO_2 and TiO_2 nanotubes, hydrothermal synthesis and formation mechanism of TiO_2 nanotubes, photocatalyst support, photoreactors, properties of phenol, and design of experiment.

2.1 Advanced Oxidation Process

Advanced oxidation processes (AOPs) represent chemical treatment procedures for carcinogenic and toxic contaminants in wastewater by oxidation (Wikipedia, 2010). The AOPs procedure is useful for the treatment of wastewater containing toxic materials such as aromatics, coloring matters, pesticides, petroleum constituents, pharmaceuticals, surfactants and volatile organic compounds (Stasinakis, 2008). AOPs have been successful in reducing the concentration of toxic chemical contaminants, hence, the cleaned wastewater can undergo to the next receiving streams or, at least, to a conventional sewage treatment (Wikipedia, 2010).

AOPs have been developed to generate highly reactive free radicals as strong oxidants by combining ozone, hydrogen peroxide, oxygen, air and UV irradiation, which showed great promise to treat the organic pollutant (Wikipedia, 2010). In 1987, Glaze et al. stated that AOPs have been developed in the water purification process to generate sufficient amount of hydroxyl radicals at ambient temperature and

pressure (Munter, 2001). The hydroxyl radical (HO·) is a non selective, powerful chemical oxidant, which acts very rapidly with most organic compounds. A list of different chemical oxidizers with its own relative oxidation potentials is given in Table 2.1. The reaction rate constants of HO· radicals with different organic compounds are also given in Table 2.2. These reaction rate constants vary in quite a wide range from 10^8 to 10^{11} $M^{-1}s^{-1}$.

Table 2.1 Oxidation Potential of Different Oxidizing Agents (Al-Kdasi et al., 2004).

Oxidizing Agent	**Electrochemical Oxidation Potential (EOP), V**
Fluorine	3.06
Hydroxyl radical	2.80
Oxygen (atomic)	2.42
Ozone	2.08
Hydrogen peroxide	1.78
Hypochlorite	1.49
Chlorine	1.36
Chlorine dioxide	1.27
Oxygen (molecular)	1.23

Table 2.2 Reaction Rate Constant (k, $M^{-1}s^{-1}$) of Hydroxyl Radical (Munter, 2001).

Organic Compound	**$K_{HO\cdot}$**
Chlorinated alkenes	10^9-10^{11}
Phenols	10^9-10^{10}
N-containing organics	10^8-10^{10}
Aromatics	10^8-10^{10}
Ketones	10^9-10^{10}
Alcohols	10^8-10^9

Once generated, HO· is aggressive in attacking virtually all organic pollutants by the common reactions, as shown in Equation 2.1-2.3. Three types of initial attack are possible: the hydroxyl radical can add itself to the organic compounds; as in the case of olefins or aromatic compounds, it can abstract a hydrogen atom from organic compounds; and as with alkanes or alcohols, it can transfer an electron from organic compounds to form hydroxyl ions (Stasinakis, 2008).

Radical addition: $R + HO\cdot \rightarrow ROH$ Equation 2.1

Hydrogen abstraction: $R + HO\cdot \rightarrow R\cdot + H_2O$ Equation 2.2

Electron transfer: $R^n + HO\cdot \rightarrow R^{n-1} + OH^-$ Equation 2.3

where R is described the reacting organic compounds.

Table 2.3 shows different methods for generating HO· radicals. Obviously, the generation of HO· is accelerated by strong oxidizing agents (O_3, H_2O_2) or combining them with catalysts (TiO_2) or radiation (UV, visible, electron-beam, ultrasonic). Of these, photocatalytic oxidation (UV/TiO_2) holds the most popular technologies for wastewater treatment (Al-Kdasi et al., 2004).

Table 2.3 Advanced Oxidation Processes (Al-Kdasi et al., 2004; Stasinakis, 2008).

Advanced Oxidation Processes	
$H_2O_2/UV/Fe^{2+}$ (photo assisted Fenton)	UV/TiO_2
H_2O_2/Fe^{2+} (Fenton)	$Ozone/TiO_2$
Ozone/UV (also applicable in the gas phase)	Sonolysis
$Ozone/H_2O_2$	Ozone sonolysis
$Ozone/H_2O_2/UV$	Supercritical water oxidation
$Ozone/TiO_2$/Electron-beam irradiation	Ozone/ultrasonics
$Ozone/TiO_2/H_2O_2$	H_2O_2/UV

In this study, only heterogeneous photocatalysis (UV/TiO_2) will be focused.

2.2 Heterogeneous Photocatalysis

Photocatalysis is a "green" technology with promising applications in a wide assortment of chemical and environmental technologies . It has been singled out as a particularly attractive means by which to oxidize and remove toxic compounds, including carcinogenic chemicals, from industrial effluent (Gupta et al., 2006). The pollutants are chemically transformed and completely mineralized to harmless compounds such as carbon dioxide, water and salts (Gupta et al., 2006). It is defined as the chemical treatment process designed to produce strong hydroxyl radicals to oxidize and remove the organic and inorganic materials in the wastewater (Thiruvenkatachari et al., 2008). Photocatalysis is a chemical process that uses light to activate a catalyst that alters the reaction rate without being involved itself. In heterogeneous photocatalysis, three main components are essential for photocatalytic reaction to take place: catalyst, light source and reactant (Thiruvenkatachari et al., 2008). According to Pirkanniemi and Sillanp□□ (2002), the overall heterogeneous photocatalysis can be summarized into the following five steps: (1) reactant diffusion to catalyst surface, (2) adsorption of reactant onto the surface, (3) chemical reaction on the catalyst surface, (4) desorption of final products off the catalyst surface and (5) diffusion of final products from the catalyst surface.

Heterogeneous photocatalysis is a favourable combination of charge transport features, electronic structures, excited-state life spans and light absorption effects. The basic of photocatalysis is the photo-excitation of a semiconductor that is solid as a result of the absorption of electromagnetic radiation, often, but not exclusively, in the near UV spectrum. When the energy (photon) supplied is equal to or greater than the band gap energy, ΔE_g of the photocatalyst, the excited electron in the valence band is transferred to the empty conduction band. (The band gap energy is the difference in energy between the valence band and conduction band of the photocatalyst. It is in the order of a few electron volts.) This leads to the generation of a positive hole (h^+) in the valence band and an electron (e^-) in the conduction band. As a result, electron-hole pairs are generated in the photocatalytic reaction. Table 2.4 shows a list of band gap energies of common semiconductors (Thiruvenkatachari et al., 2008).

Table 2.4 Band Gap Energies for Some Semiconductors At 0 K (Thiruvenkatachari et al., 2008).

Semiconductors	**Band Gap Energy (eV)**	**Semiconductors**	**Band Gap Energy (eV)**
Diamond	5.40	CdS	2.42
ZnS	3.60	ZnO	3.44
TiO_2	3.03	SnO_2	3.54
CdSe	1.70	WO_3	2.76
Si	1.17	Ge	0.74
Fe_2O_3	2.30	PbS	0.29
ZrO_2	3.87	Cu_2O	2.17

Generally, the positive hole reacts with either surface-bound water or pollutant to produce hydroxyl radical (HO·). On the other hand, the electron in the conduction band is picked up by an electron acceptor such as oxygen to produce superoxide radical anion ($O_2 \cdot^-$). The mechanism of photocatalytic reaction is shown in Equation 2.4-2.8 (Thiruvenkatachari et al., 2008):

$$\text{Photocatalyst} + hv \rightarrow e^- \text{(conduction band)} + h^+ \text{(valence band)} \quad \text{Equation 2.4}$$

where hv is energy required to transfer the excited electron from the valence band to the empty conduction band.

In this reaction, the positive hole (h^+) and electron (e^-) are powerful oxidizing and reducing agents respectively. The oxidative and reductive reactions are expressed as:

$$\text{Oxidative reaction:} \quad h^+ + H_2O \rightarrow HO\cdot + H^+ \quad \text{Equation 2.5}$$

$$\text{Reductive reaction:} \quad e^- + O_2 \rightarrow O_2 \cdot^- \quad \text{Equation 2.6}$$

Basically, the oxidative and reductive reactions do not occur concurrently. Hence, when an accumulation of electrons occurs in the conduction band, the electrons are then recombined with the positive holes in the absence of the photocatalyst. As the photocatalytic reaction proceeds in preference to the positive hole-electron recombining, efficient electron consumption is hence essential to promote the photocatalytic oxidation. The equation of the recombination of positive hole and electron is shown below:

$$e^- + h^+ \rightarrow \text{heat} \quad \text{Equation 2.7}$$

Thus, the organic pollutant is oxidized to form salts, carbon dioxide and water in the complete photocatalytic oxidation process.

$HO\cdot$ + organic pollutant + O_2 → products (salts, CO_2, H_2O) Equation 2.8

Practically all kinds of toxic chemicals are degradable by photocatalytic oxidation. Halogenated hydrocarbons are readily mineralized. Aromatic molecules are also quantitatively oxidized. In short, the carbon-containing pollutants are completely yielding carbon dioxide while the other elements bonded to the pollutants are converted to anions such as nitrate, sulphate or chloride as final products (Sin, 2009). The list of organic pollutants that can be degraded by heterogeneous photocatalysis is shown in Table 2.5.

Table 2.5 Review of Heterogeneous Photocatalytic Studies of Organic Compounds.

Organic Compounds	**Example**	**References**
Dyes	Rhodamine B	(Xiao et al., 2008; Wang et al., 2009)
	Acid Blue 25	(Mahmoodi and Arami, 2009)
	Basic dye 10	(Lee et al., 2007)
	Methyl orange	(Liao et al., 2011)
	Basic violet 3	(Gupta et al., 2006; Lee et al., 2008b)
	Methyl red	(Gupta et al., 2006)
	Acid orange 7	(Paramasivam et al., 2008)
	Reactive black 5	(Aguedach et al., 2005; Kritikos et al., 2007)
	Reactive yellow 145	(Aguedach et al., 2005; Brosillon et al., 2008)
	Malachite green dye	(Prado and Costa, 2009)
	Methylene blue	(Hsu et al., 2008)
Phenolic compounds	Phenol	(Cotto et al., 2009; Silva and Faria, 2009; Zainudin et al., 2010)
Carboxylic acids	Malic acid	(Herrmann et al., 1997)
Halophenols	Chlorophenol	(Kim et al., 2005)
	4-nitrophenol	(Kashif and Feng, 2009)
Ketones	Acetone	(Yu et al., 2006a; Yu et al., 2006b; Yu et al., 2007a; Yu et al., 2007b)
Aromatics	Toluene	(Hsu et al., 2008)
Haloalkenes	1-hexadecene	(Hsu et al., 2008)
	Propylene	(Zhang et al., 2004)
	Trichloroethylene	(Yamazaki et al., 2001; Farooq et al., 2009)

2.3 Titanium Dioxide (TiO_2) as Photocatalyst

Titanium dioxide (TiO_2) has been widely used in heterogeneous photocatalysis due to its cheap, high photocatalytic activity, non-toxicity, large stability to light illumination and stable physicochemical property (Thiruvenkatachari et al., 2008; Xiong et al., 2010). The chemical and physical properties of titanium dioxide are listed in Table 2.6.

Table 2.6 Chemical and Physical Properties of Titanium Dioxide (TiO_2) (Wikipedia, 2010).

Titanium Dioxide	
IUPAC name	Titanium dioxide, titanium (IV) oxide
Other names	Titania, anatase, rutile, brookite
Molecular formula	TiO_2
Molecular weight	79.866 g/mol
Density	4.23 g/cm^3
Melting point	1843 °C
Boiling point	2972 °C

Titanium dioxides have three common crystal forms: anatase, brookite and rutile (Nam and Han, 2003). The crystal structures of anatase, brookite and rutile are shown in Figure 2.1. Anatase and rutile are the most widely used phases of TiO_2 in industries, while reports on brookite are still rare due to its application limits. Among these, anatase phase has the photocatalytically most active modification of TiO_2, thus it acts not only as a catalyst support, but also acts as a catalyst or photocatalyst (Nam and Han, 2003). In addition, the triangular arrangement of the oxygen ions on the exposed crystal surface of anatase creates a favourable absorption condition with the organic compounds, whereas the location of titanium ions shows the effective reaction with the absorbed organics. The rutile phase, on the other hand, has higher

thermodynamic stability than the others (Nam and Han, 2003). The presence of rutile phase leads to wide pore size distribution and mesoporosity of TiO_2.

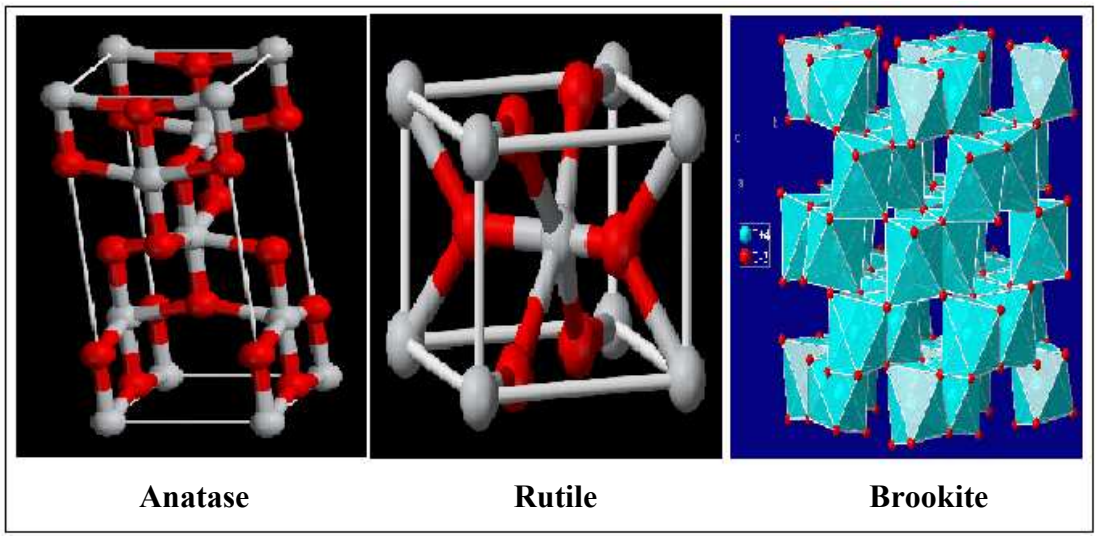

Figure 2.1 Crystal Structures of Anatase, Brookite and Rutile (Wikipedia, 2010).

2.3.1 TiO_2 Assisted Photocatalysis

The UV light is absorbed by TiO_2 during the photocatalytic process. In the UV/TiO_2 process, a redox reaction is established in the aqueous solution (Stasinakis, 2008). An excited electron in the valence band is transferred to the empty conduction band. This leads to the generation of a positive hole (h^+) and an electron (e^-) in the valence band and conduction band, as shown in Figure 2.2 (pathway A). As a result, electron-hole pairs are generated in the photocatalytic reaction (Equation 2.9).

$$TiO_2 + h_v\,(UV) \rightarrow \quad TiO_2\,(e^- + h^+) \qquad \text{Equation 2.9}$$

where h_v is energy required to transfer the excited electron from the valence band to the empty conduction band.

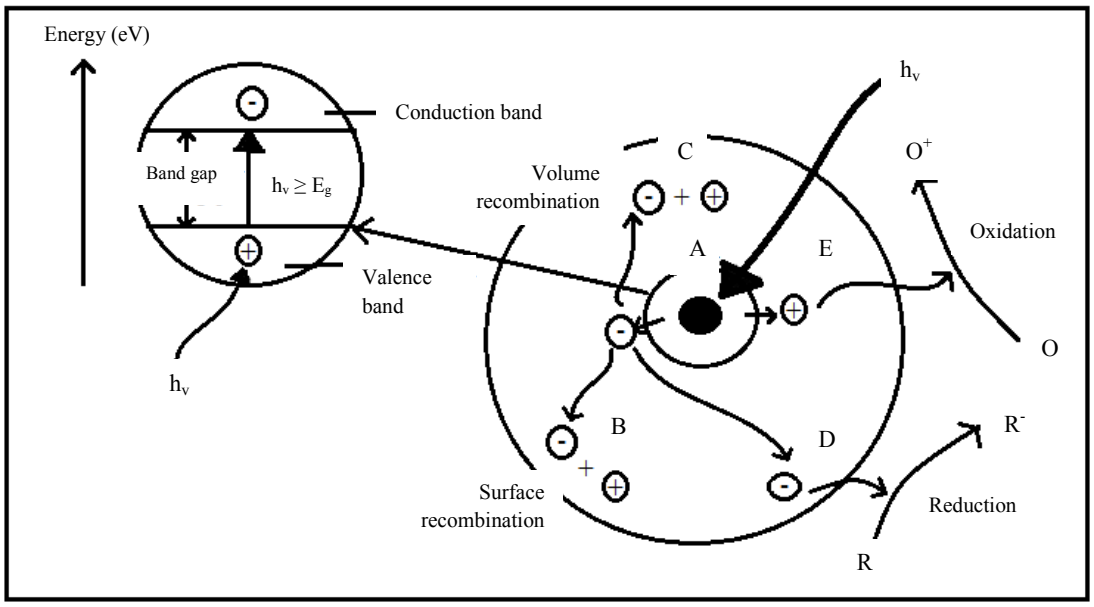

Figure 2.2 Schematic Diagram of the Photocatalytic Process Upon Irradiation of TiO_2 Semiconductor (Akpan and Hameed, 2009).

In this reaction, the recombination of the positive hole (h^+) and electron (e^-) can be occurred on the TiO_2 surface (pathway B) or in the volume of TiO_2 (pathway C). Thus, the recombination reaction must be prevented if a photocatalytic reaction must be favoured.

The activated electron will react with an oxidant to form a reduced product (pathway D) whereas the photogenerated hole will react with a reducing agent to produce an oxidized product (pathway E). The photogenerated hole can oxidize the organic molecules to form O^+, or react with OH^- or H_2O to form hydroxyl radicals ($HO\cdot$) (Equation 2.10-2.12).

$$\text{Phenol} + TiO_2\ (h^+) \rightarrow \text{oxidation products}\ (O^+) \qquad \text{Equation 2.10}$$

$$TiO_2\ (h^+) + H_2O \rightarrow \quad TiO_2 + HO\cdot + H^+ \qquad \text{Equation 2.11}$$

$$TiO_2\ (h^+) + OH^- \rightarrow \quad TiO_2 + HO\cdot \qquad \text{Equation 2.12}$$

The electron can reduce the organic molecules to form R^-, or interact with surface adsorbed molecular oxygen (O_2) to form superoxide radical anions ($O_2\cdot^-$) (Equation 2.13-2.15).

$$\text{Phenol} + TiO_2\,(e^-) \rightarrow \text{reduction products } (R^-) \qquad \text{Equation 2.13}$$

$$TiO_2\,(e^-) + O_2 \rightarrow \quad TiO_2 + O_2\cdot^- \qquad \text{Equation 2.14}$$

$$O_2\cdot^- + H^+ \rightarrow \quad HO_2\cdot \qquad \text{Equation 2.15}$$

At the end of the photocatalytic process, the phenol is oxidized with the resulting HO· radicals to form salts, carbon dioxide and water.

$$HO\cdot + \text{phenol} \rightarrow \quad \text{degradation products (salts, } CO_2, H_2O) \qquad \text{Equation 2.16}$$

2.3.2 Nanostructured TiO_2

Since the photocatalytic reaction is affected by adsorption of the substrate on TiO_2 surface, the physical and chemical properties of photocatalyst that determine its morphology, dimension and crystallite phase is important in photocatalytic degradation reaction. Recent researches have been taken that many of the difficulties involving wastewater treatment could be greatly improved using different titanate nanostructures with the aim of increasing photocatalytic efficiency (Costa and Prado, 2009; Okour et al., 2009).

Nanostructured materials such as nanofibers, nanoparticles, nanorods, nanospheres, nanotubes and nanowires present new features and opportunities for enhanced performance in many promising applications (Wang et al., 2007; Wang et al., 2008a; Costa and Prado, 2009; Seo et al., 2009). Nanostructured materials are of special significance owing to their excellent physicochemical properties that are catalytic, electronic, magnetic, mechanical and optical in nature (Poudel et al., 2005). They are widely applied in air and water purification technologies, photocatalysis, gas sensors, high effect solar cells and microelectronic devices (Nakahira et al., 2004; Yu and Yu, 2006). For example, O'Regan et al. stated that titania nanotubes have been used in high quality, efficient solar cells (Nakahira et al., 2004). Nanostructured materials with different morphologies have varying specific properties, and hence, the new applications of such materials are related to the shape and size of the nanostructured materials (Wang et al., 2007). The synthesis of nanostructured materials with specific shape and size, as well as the understanding of their formation mechanism are two important research aspects in material science and technology (Wang et al., 2007). Nanowires, nanotubes and nanofibres of TiO_2 have been successfully prepared by electrochemical synthesis, template based synthesis and a chemical based route although the effectiveness and practicality of some of these materials as photocatalysts are still being evaluated (Yu and Yu, 2006; Okour et al., 2009).

2.3.3 TiO_2 Nanotubes

The discovery of the carbon nanotubes in the 1990s by Iijima opened new fields in the material science sector (Costa and Prado, 2009). Nanotubular materials are considered important in photocatalysis owing to their special electronic and mechanical properties, high photocatalytic activity, large specific surface area and high pore volume (Idakieva et al., 2005; Yu and Yu, 2006). Several studies have shown that titania nanotubes have better physical and chemical properties in photocatalysis compared with other forms of titanium dioxide. For example, titania nanotubes have a relatively higher interfacial charge transfer rate and surface area compared with the spherical TiO_2 particles (Colmenares et al., 2009). The transfer of the charge carriers along the length of titania nanotubes can reduce the recombination of positive hole and electron (Colmenares et al., 2009). Li et al. (2009) found that hollow titania nanotubes were highly efficient in the photocatalytic decomposition of methyl orange compared with rutile phase TiO_2 nanopowders. Xu et al. (2006) stated that titania nanotubes were excellent photocatalysts, which were more reactive than TiO_2 nanopowder (anatase P25) in long cycles.

Thus, titania nanotubes have raised expectations in what nanotechnology can achieve because of their interesting microstructure and potential photoelectrochemical applications in dye-sensitized solar cells, gas sensors, organic light-emitting diodes and photocatalysts (Yu et al., 2007b). Considerable effort is now being devoted to the production of well-structured TiO_2 nanotubes with novel properties such as high surface area and pore volume (Idakieva et al., 2005).